

---

# FAST PATH PLANNING ALGORITHMS FOR UNMANNED AERIAL VEHICLES

---

A PREPRINT

**Mohammad Reza Ranjbar Divkoti**  
Department of Computer Engineering  
Ferdowsi University of Mashhad  
Mashhad, Iran

mohammadreza.ranjbardivkoti@mail.um.ac.ir

**Mostafa Nouri-Baygi\***  
Department of Computer Engineering  
Ferdowsi University of Mashhad  
Mashhad, Iran

nouribaygi@um.ac.ir

April 28, 2019

## ABSTRACT

Path planning is a major problem in autonomous vehicles. In recent years, with the increase in applications of Unmanned Aerial Vehicles (UAVs), one of the main challenges is path planning, particularly in adversarial environments. In this paper, we consider the problem of planning a collision-free path for a UAV in a polygonal domain from a source point to a target point. Based on the characteristics of UAVs, we assume two basic limitations on the generated paths: an upper bound on the turning angle at each turning point (maximum turning angle) and a lower bound on the distance between two consecutive turns (minimum route leg length).

We describe an algorithm that runs in  $O(n^4)$  time and finds a feasible path in accordance with the above limitations, where  $n$  is the number of obstacle vertices. As shown by experiments, the output of the algorithm is much close to the shortest path with this requirements. We further demonstrate how to decompose the algorithm into two phases, preprocessing time and query time. In this way, given a fixed start point and a set of obstacles, we can preprocess a data-structure of size  $O(n^4)$  in  $O(n^4)$  time, such that for any query target point we can find a path with the given requirements in  $O(n^2)$  time. Finally, we modify the algorithm to find a feasible (almost shortest) path that reach the target point within a given range of directions.

**Keywords** Path planning · Unmanned aerial vehicles · Polygonal domains · Maximum turning angle · Minimum route leg length

## 1 Introduction

An Unmanned Aerial Vehicle (UAV), is a flying machine without a human pilot. Due to its advantages in military, civil and industrial markets, they are largely employed in situations dangerous for human life [22, 8, 5]. Since traditional remote piloting are not adequate for current complex missions, autonomous path planning are utilized extensively for UAVs [7].

Path planning is the problem of finding a feasible path from a given source to a given target for a moving object, that optimizes a desirable objective function and taking into account different constraints. The constraints are of various types, for example, non-accessible points in the space, velocity and acceleration constraints, uncertainty about the environment and so on. This problem in its generic form is NP-hard [1] and has polynomial time algorithms only in some special cases [10].

This problem has been extensively studied in robotics and various algorithms are presented for different forms of it. In general, the problem of path planning in robotics is more complex than in UAVs because of high degrees of freedom.

---

\*Corresponding author

For example, articulated robots can move their arms, or the shapes of some robots are too complex, and the robots must move in several directions to be able to pass through some regions in the environment (Piano Mover's Problem [19]).

In contrast to the robot path planning, the UAV path planning has several characteristics. The three major differences in path planning for UAVs are as follows. First, due to the small size of the flying object compared to the space, we usually model a UAV as a moving point in the space. This makes the problem of path planning much simpler.

Second, because of the high speed of UAVs, it is not possible for a UAV to rotate at a sharp angle in its flight path [31, 23]. This is completely different from a robot's movement in which the robot can slow down or even stop to rotate. Because of this, the flight path of a UAV must be smooth and the path planner should avoid sharp turns. This limitation makes the path planning for UAVs different compared to the conventional path planning for robots, and increases the complexity of the path planner. The complexity magnified when the number of obstacles increases and the path planner may have to create a longer zigzag path with many rotations in order to make a smooth path. In addition to the limit on the turning angles, usually a UAV cannot have two consecutive turns in a short time. This enforces the path planner to make enough distance between two successive turns [31, 23].

The third difference in the UAV path planning is the ability of a UAV to change its flight height. Robots usually move on the surface of the earth, so the problem of robot path planning is normally defined on the plane. But given the fact that UAVs fly in the space, and sometimes there is a need for a change in altitude to avoid obstacles (for example, a UAV flying over a terrain, or a cruise missile over a sea near scattered islands). In these cases, the problem of designing a path should be solved in a three-dimensional space which introduces new complexities [12, 20, 27].

In this paper, we consider the first and second characteristics of UAVs path planning, and, as will be explained later, we design a smooth path for a moving point among polygonal obstacles. However, due to the complexity of the path planning problem in three-dimensional space, we choose the two-dimensional space for path planning in this paper and defer the three-dimensional case to later work.

The UAVs path planning algorithms are divided into two general categories, offline and online, based on the knowledge of the planner about the environment. A path planning algorithm is called offline, if the designer has complete information about the environment and obstacles in it [12, 15, 26]. On the other hand, an online algorithm knows little or nothing at all about the environment in which the movement will take place [25, 24, 15]. In the latter case, the path planning is done while the UAV moves and based on the information we get from the sensors, the path is corrected. In this paper we choose to work on offline algorithms.

In terms of the number of reported paths, the algorithms can be divided into three categories. In the first category, the path planning is performed only for one device. Most algorithms are included in this category. In the second category, the path planning is done simultaneously for a set of UAVs. In some applications, for example a salvo attack against a warship, in order to prevent air defence systems activation, target missiles must simultaneously hit the same target with different angles. In this case, the path planner algorithm finds the best paths for several UAVs all at once [29, 21, 9, 13]. In the third category, the path planning is performed for different targets, while the environment and the source point are fixed. This type of algorithms are useful when the target point is moving and we want to find the best time/place of the target to reach it, by taking advantage of fixed environment to speed up the path planning.

In this paper, we first propose a path planner algorithm for a single UAV. Later, with some changes, we split the algorithm into a preprocessing phase and a query phase in order to be able to find paths for multiple targets in a much shorter time.

In terms of the shape of the path, the algorithms are divided into two classes. In the first one, the output of the algorithm is composed of straight line segments that are connected together [6, 23, 31]. In the second class, the output consists of straight line segments and more complex curves such as arcs [20], Bezier curves [28, 21, 27] and B-Spline curves [12, 14]. The advantage of the former is the simplicity of the path and the speed of the path planner, while the latter is better to adapt to the rotation limitations of UAVs and not having sharp angle rotations. In contrast, the latter algorithms have high execution time and are rarely applicable in practice.

Based on the limitations described above that we consider for the path, we have the simplicity and speed of line segment path planners, while at the same time smoother paths are obtained that are traversable by UAVs.

The two limitations used in this paper, were also previously considered by other researchers. *Szczerba et al.* [23] were the first who described these two limitations. They used a heuristic search algorithm to find a path in the two-dimensional space with the above limitations that has length not more than a fixed given value and approaching the target from a desirable direction (approximately). The main problem with their algorithm, as will be explained in Section 6, is its running time. Later *Zheng et al.* [30] and *Zheng et al.* [31] considered the problem in the three-dimensional space and added two new limitations to the path, namely minimum flying height and maximum climbing/diving angle.

They used an evolutionary algorithm to solve the problem, which as Szczerba *et al.*'s algorithm [23] has high running time when the complexity of the environment grows.

## 1.1 Our results

We can summarize our results as follows:

- We present an offline, graph based path planning algorithm, called RCS. We first make two assumptions about the required path, and then create a graph which models feasible paths with those requirements, and finally apply Dijkstra's algorithm [4] on this graph to find the shortest path from the source node to the target node. Because we find the shortest path with these properties, as we show in experimental results, the length of the result of the algorithm is much close to the length of the optimum path.
- We prove an upper bound on the time and space complexity of RCS. We show that if all inputs of the problem is given at the same time to the algorithm, we can solve the problem in  $O(n^4)$  time and  $O(n^4)$  space. In these upper bounds  $n$  is the number of obstacle vertices.
- For another version of the problem, in which several UAV's need to be launched from a fixed source, or we need to find the best time/path to reach a moving target point, we can divide the RCS algorithm into two phases, such that given the set of obstacles and the source point, we preprocess a data structure of  $O(n^4)$  size in  $O(n^4)$  time, and for any query target point we can find the result in  $O(n^2)$  time.
- We change the RCS algorithm in such a way to find the best path that approaches the target point from a direction within a specified range of directions. The running time and the space usage of the algorithm do not change.

A preliminary version of this paper is presented in the 7th International Conference on Computer and Knowledge Engineering [18]. This paper extends that by giving a complete literature review, considering an extension of the problem in Section 5.2, and presenting a thorough evaluation of the algorithms.

The remaining of the paper is organized as follows: The problem is formally described in Section 2. In Section 3, we discuss the geometrical concepts needed to solve the problem. We present the algorithm to solve the problem in Section 4. The extensions of the algorithm are described in Section 5 and the experimental evaluations are presented in Section 6. Section 7 concludes the paper.

## 2 Problem Description

We here formally define the problem. In the plane, a set  $O = \{P_1, P_2, \dots, P_h\}$  of  $h$  disjoint simple polygons, called obstacles, which totally have  $n$  vertices, a source point  $s$ , a target point  $t$  and two constant values  $l$  and  $\alpha$  are given. Our goal is to find a path in the exterior space of polygons of  $O$ , called the free space, from  $s$  to  $t$  with the following properties:

- *Minimum route leg length*: the path consists of straight line segments, each of length at least  $l$ .
- *Connectedness*: the consecutive segments are connected at turning points.
- *Maximum turning angle*: the turning angles at the turning points are at most  $\alpha$ .

Figure 1 depicts a set  $O = \{P_1, P_2, P_3\}$  of three obstacles, with  $n = 14$  vertices, source point  $s$  and target point  $t$ . Each path from  $s$  to  $t$  is composed of a chain of segments. The illustrated path  $\{e_1, e_2, e_3\}$  in the figure have the above properties if  $l \leq |e_1|, |e_2|, |e_3|$  and  $\theta_1, \theta_2 \leq \alpha$ .

## 3 Preliminaries

In this section, we introduce some geometric tools used for solving the problem. In Section 3.1 we define a regular chain of segments and in Section 3.2 the ray shooting data structure is briefly explained.

### 3.1 Regular chain of segments

In our problem we consider only paths consisting of a sequence of connected line segments. We call such a sequence a *chain of segments*. Each two consecutive segments have a common endpoint, called the *turning point*. The angle

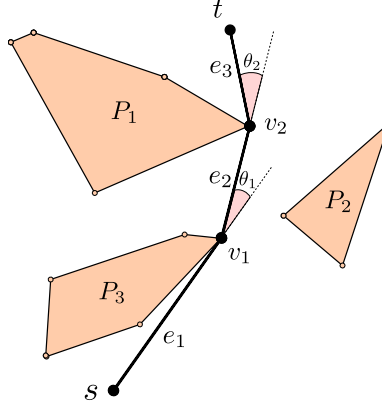


Figure 1: Path planning in the presence of polygon obstacles, with *connectedness*, *minimum route leg length*, and *maximum turning angle* properties.

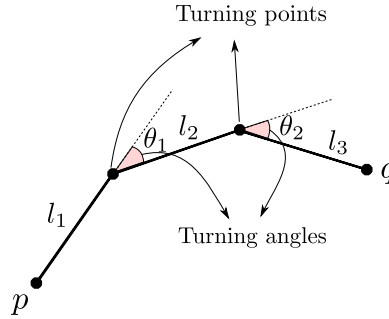


Figure 2: chain of segments from  $p$  to  $q$  with condition  $l_1, l_2, l_3 \leq l, \theta_1, \theta_2 \leq \alpha$ .

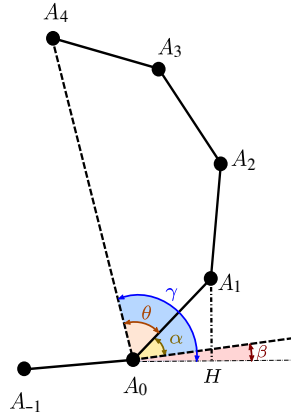


Figure 3: A regular chain of segments from point  $A_0$  to  $A_4$  with three turning points.

between a segment and the extension of the previous segment in the turning point is called the *turning angle*. (Figure 2)

We call a chain of segments with all turning angles equal to  $\alpha$  and equal leg lengths a *regular chain of segments*. Intuitively, it is part of a regular polygon with exterior angle  $\alpha$ .

We here calculate the position of vertices of a regular chain of segments with different number of turning points, while the position of the start and the end points are known.

Let  $C$  denote a regular chain of segments with  $A_0$  as the starting point,  $A_{k+1}$  as the end point, and with  $k$  turning points. We assume the  $x$ -axis is the rightward horizontal line through the origin and the  $y$ -axis the upward vertical line through the origin. Let  $A_i, 1 \leq i \leq k$ , be the  $i^{\text{th}}$  turning point of  $C$ . Let  $e$  denote the length of the segments of  $C$ . For

ease of illustration, we consider  $A_0$  as an imaginary turning point and denote its previous point by  $A_{-1}$  (Figure 3). Let  $\beta$  denote the angle between the extension of  $\overline{A_{-1}A_0}$  and the  $x$ -axis. Since  $C$  is a regular chain of segments, the angle between the extension of  $\overline{A_{-1}A_0}$  and  $\overline{A_0A_1}$  is  $\alpha$ . Let the angle between  $\overline{A_0A_1}$  and  $\overline{A_0A_{k+1}}$  (the direct line segment from the starting point to the end point) be denoted by  $\theta$ .

Draw a line from  $A_0$  parallel to the  $x$ -axis and project  $A_1$  on this line. Let  $H$  denote the projection point (Figure 3). In the right triangle  $\triangle A_0HA_1$  we have

$$x_{A_1} - x_{A_0} = |A_0A_1| \cos(\alpha + \beta),$$

$$y_{A_1} - y_{A_0} = |A_0A_1| \sin(\alpha + \beta).$$

Similarly, we can draw a horizontal line through  $A_1$  and project  $A_2$  on this line and get the following equations

$$x_{A_2} - x_{A_1} = |A_1A_2| \cos(2\alpha + \beta),$$

$$y_{A_2} - y_{A_1} = |A_1A_2| \sin(2\alpha + \beta).$$

As it follows, the position of each point  $A_i$ , can be calculated from the following recurrence relations

$$x_{A_i} - x_{A_{i-1}} = |A_{i-1}A_i| \cos(i\alpha + \beta),$$

$$y_{A_i} - y_{A_{i-1}} = |A_{i-1}A_i| \sin(i\alpha + \beta).$$

Since  $e = |A_{i-1}A_i|$ , for all  $1 \leq i \leq k+1$ , we solve the above recurrence relations as follows

$$x_{A_j} = e \sum_{i=1}^j \cos(i\alpha + \beta) + x_{A_0}, \quad (1)$$

$$y_{A_j} = e \sum_{i=1}^j \sin(i\alpha + \beta) + y_{A_0}, \quad (2)$$

where  $j = 1, \dots, k+1$ .

In a simple polygon, the sum of the interior angles with  $d$  vertices is equal to  $(d-2)\pi$ . If we connect  $A_0$  to  $A_{k+1}$ , we have a simple polygon. In this polygon, the interior angle at  $A_0$  and  $A_{k+1}$  are equal, because  $C$  is part of a regular polygon. Let  $d$  be the number of vertices of the polygon. Since  $k$  is the number of turning points in  $C$ , we have  $k = d - 2$  and so the sum of the interior angles of the simple polygon is  $(d-2)\pi = k\pi$ . The interior angle of the first and the last vertices in the chain is  $\theta$  and the other angles are  $\pi - \alpha$ . Therefore we have  $k(\pi - \alpha) + 2\theta = k\pi$ , or equivalently  $\theta = \frac{k\alpha}{2}$ .

Let the angle between  $\overline{A_0A_{k+1}}$  and the  $x$ -axis be denoted by  $\gamma$ . If we know the position of  $A_0$  and  $A_{k+1}$ , we have the value of  $\gamma$ . Since  $\gamma = \beta + \alpha + \theta$ , we can rewrite this equation to have  $\beta$  on the left hand side as  $\beta = \gamma - (\alpha + \theta)$ . Therefore, we have the value of  $\beta$ . If we further know the number of turning points of  $C$ , i.e.  $k$ , the length of segments of  $C$  can be computed with each of the following equations

$$e = \frac{x_{A_{k+1}} - x_{A_0}}{\sum_{i=1}^{k+1} \cos(i\alpha + \beta)} = \frac{y_{A_{k+1}} - y_{A_0}}{\sum_{i=1}^{k+1} \sin(i\alpha + \beta)}.$$

Obtaining the value of  $e$ , the position of each vertex in the chain will be identified by Equations 1 and 2.

With the above method, given the starting and the end points and the number of turning points, we can easily determine the position of the turning points of the regular chain of segments.

### 3.2 Ray shooting

One of the problems we encounter for path planning is to recognize if a segment intersects a set of segments. Formally, given a set of segments  $S = \{s_1, s_2, \dots, s_n\}$ , we are asked if segment  $t$  intersects at least one of the segments of  $S$ .

It is obvious that this problem could be solved by checking the intersection of the segment  $t$  with all the segments of  $S$  in  $\Theta(n)$  time. But, since the problem must be solved a lot of times for a fixed given set of segments, an algorithm with less query time is more desirable. We use ray shooting algorithms for this problem. In the ray shooting problem, a set of segments  $S$  is known. We need to preprocess  $S$  such that given a query ray (its start point and direction), the first intersection position of the ray with the segments of  $S$  will be recognized quickly. We should also detect the case in which the ray does not intersect any segment of  $S$ .

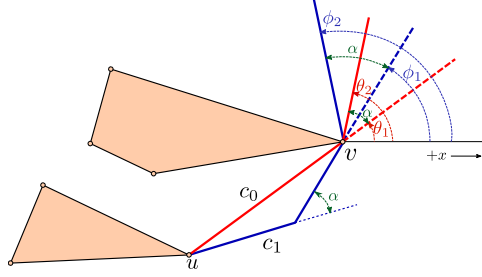


Figure 4: Following the chain  $c_0$ , where the object moves directly towards  $v$ , it can leave  $v$  in a direction in the range  $\text{VLR}(c_0) = [\theta_1, \theta_2]$ , while for the chain  $c_1$  the valid leaving range of directions is  $\text{VLR}(c_1) = [\phi_1, \phi_2]$ .

By the solution of this problem, the problem of segment intersection with a set of segments will be solved as follow: first, we preprocess  $S$  for solving the ray shooting problem. During the query time by receiving the segment  $t$ , we shoot a ray from one end-point of  $t$  in the direction of the other end-point. If the first intersection point between this ray and the segments of  $S$  is between the end-points of  $t$ , the answer to our solution is positive, in other words,  $t$  has intersection with the segments of  $S$ . On the other hand, if the intersection point is not between the end-points of  $t$  or there is not any intersection at all, the answer to our problem is negative.

Different algorithms are suggested for the ray shooting problem. The last results belong to Chan [2] and Chen and Wang [11]. Chan [2] introduced a randomized algorithm which after preprocessing in  $O(n \log^3 n)$  time and using  $O(n \log^2 n)$  space solves the problem of ray shooting for an arbitrary query ray in  $O(\sqrt{n} \log^2 n)$  average time. Chen and Wang [3] constructed a data structure of size  $O(n + h^2)$  in  $O(n + h^2 \log^c n)$  time that answer the ray shooting queries in  $O(\log n)$  time. In the preprocessing time bound above,  $c$  is a constant.

By combining the latest results about the ray shooting problem and the technique used by Matouek [11] we conclude that for any arbitrary parameter  $b$ , where  $n \log^2 n \leq b \leq n^2$  and a constant  $c$ , a data structure of size  $O(b)$  can be constructed in  $O(b \log^c n)$  preprocessing time such that the problem of ray shooting for any arbitrary query segment can be solved in  $O((\frac{n}{\sqrt{b}}) \log^c n)$  time.

## 4 RCS: Path Planning Algorithm

In this section, we describe our algorithm for finding a path with the given requirements. Since we prefer to make the path smooth, we try to spread out the break points along the path evenly. Therefore, we use regular chains of segments when moving from an obstacle vertex to another one, and so we call our algorithm *Regular Chains of Segments Path Planner*, or simply *RCS*.

Let  $u$  and  $v$  be two obstacle vertices. We want to find all paths starting from  $u$  to  $v$  not passing through other vertices of obstacles. To do this, we examine all regular chains of segments with different number of break points starting from  $u$  and ending at  $v$ . If all edges of a chain do not intersect any edges of the obstacles, then the desired chain is considered as a *valid* path from  $u$  to  $v$ . In other words, we first look at the regular chain of segments without any break point, that is the straight line segment from  $u$  to  $v$ . If the only edge of this chain does not intersect any obstacle then we consider this chain as a valid path from  $u$  to  $v$ . Similarly, we examine the regular chain of segments with one break point, two break points, and so on. We continue this process until the distance between two adjacent break points in the chain gets smaller than  $l$ . If the first and the last points of a regular chain are fixed, the distance between two consecutive break points decreases when the number of break points increases. Therefore there are a limited number of valid regular chains of segments from  $u$  to  $v$ .

Assume the moving object follows a given regular chain of segments from  $u$  to  $v$  when traveling from the start point to the target. Because of the “maximum turning angle property”, when the object moves away from  $v$ , its *leaving direction* must be within a fixed range. This observation is depicted in Figure 4. Following the chain  $c_0$ , where the object moves directly towards  $v$ , it can leave  $v$  straight and without any rotation at  $v$ , or rotate at an angle at most equal to  $\alpha$ . Therefore, the object leaves  $v$  in a direction in the range  $[\theta_1, \theta_2 = \theta_1 + \alpha]$ . Similarly, for the chain  $c_1$  with a single break point, the valid leaving direction is in the range  $[\phi_1, \phi_2 = \phi_1 + \alpha]$ ;  $\phi_1$  is the angle of the path if the object does not rotate at  $v$ , and  $\phi_2$  is the angle of the path when the object rotate at angle equal to  $\alpha$ . We call this range, the valid leave range of the chain  $c$ , and denote it by  $\text{VLR}(c)$ .

In the following, we construct a graph  $\mathcal{G} = (V_{\mathcal{G}}, E_{\mathcal{G}})$ , such that the shortest path between two vertices in  $\mathcal{G}$  corresponds to the shortest path from the starting point  $s$  to the target point  $t$  in the original configuration, consisting only of regular

chains of segments. In order to find the shortest path in  $\mathcal{G}$  we use Dijkstra's algorithm [4]. For an obstacle vertex  $v$  and a valid leaving range  $r = [\theta_1, \theta_2]$ , we add a node  $v_r$  to  $\mathcal{G}$ . In addition, for each pair  $u_r$  and  $v_{r'}$  of nodes in  $\mathcal{G}$ , if the following conditions hold, we add an edge from  $u_r$  to  $v_{r'}$ .

1. There exists a regular chain of segments  $c$  from  $u$  to  $v$ .
2. The chain  $c$  does not intersect any obstacle.
3. It leaves  $u$  in a direction in the range  $r$ .
4.  $\text{VLR}(c) = r'$ .

The weight of this edge is equal to the length of  $c$ .

Now let's explain how to construct the graph. We add the starting point  $s$  and the target point  $t$  to the set of obstacle vertices. We have a set of unprocessed graph nodes, denoted by  $U_{\mathcal{G}}$ , which initially contains only node  $s_{[0,2\pi]}$ , corresponding to vertex  $s$  with a full range of valid leaving directions. During the construction of  $\mathcal{G}$ , we remove a node  $u_r$  from  $U_{\mathcal{G}}$  and find all valid regular chains we could draw from vertex  $u$  to all other obstacle vertices which leave  $u$  in directions in the range  $r$ . For each valid chain  $c$  with this property from  $u$  to a vertex  $v$ , let  $r' = \text{VLR}(c)$ . We add a new node  $v_{r'}$  to  $U_{\mathcal{G}}$ , which must be processed later and added to  $\mathcal{G}$ . We also add an edge to the set of edges of  $\mathcal{G}$  from node  $u_r$  to node  $v_{r'}$  corresponding to  $c$ . Finally, when  $u_r$  is processed completely, we add it to  $V_{\mathcal{G}}$ , which is the set of vertices of  $\mathcal{G}$ . We repeat this process until there is no node in  $U_{\mathcal{G}}$ .

**Lemma 1.** *For a polygonal domain of  $n$  vertices the number of nodes of  $\mathcal{G}$ ,  $|V_{\mathcal{G}}|$ , is  $O(\frac{2\pi}{\alpha}n^2)$  and the number of edges,  $|E_{\mathcal{G}}|$ , is  $O(|V_{\mathcal{G}}|^2)$ .*

*Proof.* For each pair of vertices  $u$  and  $v$ , we have at most  $\frac{2\pi}{\alpha} + 1$  valid regular chains of segments. This is because the maximum number of break points is  $\frac{2\pi}{\alpha}$ . For a vertex  $v$  and a valid chain  $c$ , a single node will be added to  $\mathcal{G}$ . Therefore, the number of nodes is at most equal to the number of different pairs of vertices times the number of valid regular chains from the first vertex to the second one, that is  $O(\frac{2\pi}{\alpha}n^2)$ .

The second claim about the number of edge of  $\mathcal{G}$  is trivial as  $\mathcal{G}$  is a simple graph. □

The above bounds for the complexity of  $\mathcal{G}$  are clearly the worst case upper bounds. This is because it is very rare that most of the chains from  $u$  to  $v$  are valid.

**Lemma 2.** *The shortest path in  $\mathcal{G}$  from node  $s_{[0,2\pi]}$  to all nodes  $t_r$  for some valid leaving range  $r$  is equal to the shortest path in the polygonal domain from vertex  $s$  to vertex  $t$  that consists of only regular chains of segments.*

*Proof.* We construct  $\mathcal{G}$  such that any valid regular chain of segments from a vertex  $u$  to a vertex  $v$  has a corresponding edge in the graph with the same weight as the length of the chain. We can establish a one to one mapping between each path in  $\mathcal{G}$  and each path in the polygonal domain which consists of only regular chains of segments. Therefore the shortest path in the plane has a corresponding path in  $\mathcal{G}$ , which is the shortest path in  $\mathcal{G}$  from  $s_{[0,2\pi]}$  to some node in  $\mathcal{G}$  related to  $t$ . □

From Lemma 2, we conclude the following corollary:

**Corollary 1.** *Applying Dijkstra's algorithm on  $\mathcal{G}$  from  $s_{[0,2\pi]}$  until we reach some node related to vertex  $t$ , solves the path planning problem in polygonal domain.*

The following theorem states the running time and space complexity of finding the shortest path problem consisting of regular chains of segments.

**Theorem 1.** *The RCS algorithm can be run in  $O(n^4)$  time using  $O(n^4)$  space, where  $n$  is the total number of obstacle vertices.*

*Proof.* The running time of Dijkstra's algorithm on a graph with  $|V|$  vertices and  $|E|$  edges is  $O(|E| + |V| \log |V|)$  using Fibonacci heap data structure. According to Lemma 1, the running time and the space usage of the algorithm on  $\mathcal{G}$  will be  $O(\frac{4\pi^2}{\alpha^2}n^4)$ . Since  $\pi$  and  $\alpha$  are constants, the claim is proved. □

## 5 Extensions

In this section we consider two extensions of the problem and try to use our technique to solve these extensions. In the first problem there are several target points that are to be processed with a single starting point, and we have to find the best path to reach each target point. In the second extension, we solve the problem assuming that we have to reach the target point with a specific range of directions.

### 5.1 Problem in the query mode

In the original problem, it was assumed that the target point  $t$  is given at the same time as the other inputs. In this section we divide the algorithm into two parts, a preprocessing phase, and a query phase. In the preprocessing phase, the set of obstacles and the starting point are given and in the query phase the target point is determined. The problem in this mode is suitable when we want to find the best time/path to reach a moving target point in a fixed environment.

We solve the problem in the query mode as follows. Given the set of obstacles and the starting point in the preprocessing phase, we construct the graph  $\mathcal{G}$  and run Dijkstra's algorithm on  $\mathcal{G}$  to find the shortest path from  $s_{[0,2\pi]}$  to all other nodes. In the query phase, given the target point  $t$ , we consider each node  $u_r$  in  $\mathcal{G}$  and find the valid regular chain of segments from  $u$  to  $t$  with the smallest number of break points which leaves  $u$  in a direction in the range  $r$ . If there exists such a chain, we add the length of the chain to the length of the shortest path from  $s_{[0,2\pi]}$  to  $u_r$  and store it as a possible path from  $s$  to  $t$ . The final solution is the shortest path among all such possible paths.

**Theorem 2.** *For the problem of path planning with “maximum turning angle”, “connectedness” and “minimum route leg length” properties, we can preprocess a data structure in  $O(n^4)$  time using  $O(n^4)$  space, to answer the query for any target point  $t$  in  $O(n^2)$  time. In these upper bounds  $n$  is the total number of obstacle vertices.*

*Proof.* We can construct the graph using  $O(n^4)$  space and run Dijkstra's algorithm in  $O(n^4)$  time as proved in Lemma 1 and Theorem 1, respectively. In the query time, we need to process each node of the graph in  $O(1)$  time to find a possible path to  $t$ . Processing all nodes and choosing the shortest path to  $t$  takes  $O(|V_{\mathcal{G}}|) = O(n^2)$  time.  $\square$

### 5.2 Approaching from a given direction

In some path planning applications, it is desirable to reach the target from a given direction. For example the most damage will take place when a missile hits the target orthogonally, or a UAV landing on an aircraft carrier needs to approach it from a fixed direction. In this section we describe how we can use the method to achieve this goal.

In this version of the problem, in addition to the previous inputs, a range of directions like  $\Theta = [\theta_1, \theta_2]$  is given, and we want to approach the target from a direction in the range  $\Theta$ .

In Section 4 we described how to construct a graph  $\mathcal{G}$  that models all valid paths only consisting of regular chains of segments and have the required properties. Each edge  $(u_r, v_{r'})$  in this graph has the following meaning: there exists a regular chain of segments  $c$  from the obstacle vertex  $u$  to the obstacle vertex  $v$  which leaves  $u$  in a direction in the range  $r$  and when the object leaves  $v$  it can follow any direction in the range  $r'$ . It is obvious that if we use this edge (meaning the moving object follows  $c$  from  $u$  to  $v$  in the path), it comes to  $v$  in a fixed direction determined by  $c$ .

Therefore, the solution is as follows. When we construct the graph, we only care about target nodes of the form  $t_{r'}$  such that the moving object can get to them at a direction in the range  $\Theta$ . For each pair of nodes  $(u_r, t_{r'})$ , if there exists a valid regular chain of segments from  $u$  to  $t$  (with the required properties), such that the chain reaches  $t$  in a direction in the desirable range, we mark  $t_{r'}$  as an appropriate candidate target node. When we run Dijkstra's algorithm on  $\mathcal{G}$ , we select the shortest path among all paths to all such marked nodes of  $\mathcal{G}$ . It is obvious that the resulting path reaches  $t$  in a direction in the desirable range.

By the above argument we conclude the following theorem:

**Theorem 3.** *In the problem of path planning with a fixed approaching direction, a path from the starting point  $s$  to the target point  $t$  with the required properties can be found in  $O(n^4)$  time using  $O(n^4)$  space, where  $n$  is the total number of obstacle vertices.*

*Furthermore, we can preprocess a data structure in  $O(n^4)$  time using  $O(n^4)$  space, to answer the query version of the problem for any target point  $t$  in  $O(n^2)$  time.*



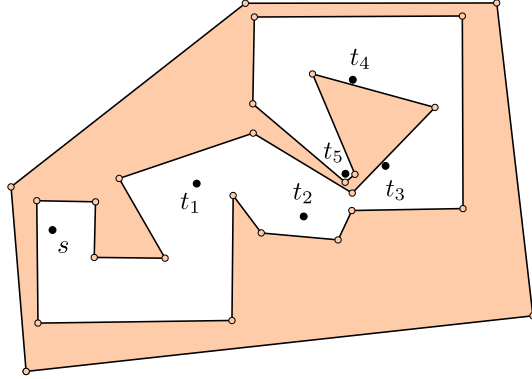


Figure 5: The scene used for the first experiment with  $\alpha = \pi/6$  and  $l = 50$ . The source point  $s$  and five different target points  $t_1, \dots, t_5$  are denoted in the figure.

Table 1: Comparison of the results of the RCS and A\* algorithms on the configuration of Figure 5

Target	RCS preprocessing time (ms)	RCS query time (ms)	RCS total time (ms)	A* running time (ms)	RCS path length	A* path length	Relative difference
$t_1$	6.28	0.26	6.54	375	487.6	470.4	3.5%
$t_2$	6.76	0.20	6.96	14183	715.5	670.2	6.3%
$t_3$	6.83	0.23	7.06	71164	998.5	952.2	4.6%
$t_4$	6.86	0.25	7.11	165713	1539.6	1467.0	4.7%
$t_5$	6.88	0.26	7.14	230670	1954.4	1860.8	4.8%

## 6 Algorithm Evaluation

Although it may seem that the running time and the space usage of the proposed algorithms are huge, it is not so because the dependency is on the number of obstacle vertices and not on the scene size. In most applications the area in which the algorithm works is extremely large. But the complexity of the scene in terms of the number of obstacle vertices is not considerable. This can be made more rigorous if we apply a simplification step on the input to decrease the number of obstacle vertices.

In this section we perform several experiments to evaluate the RCS algorithm and show its effectiveness in practice. We compare the results to the results of the algorithm designed by Szczerba *et al.* [23]. We chose their algorithm because they solved the most similar problem to the problem considered in this paper. Their algorithm is based on the A\* search algorithm, and we called it A\* hereinafter. The evaluations are performed based on seven test cases. The source codes of the RCS and A\* algorithms are available at the GitHub repository hosting service [17, 16].

In the first experiment, we run RCS and A\* on a fixed complex polygonal domain from a given source point to several target points. The configuration is depicted in Figure 5. In this figure,  $s$  is the source point and  $t_1, \dots, t_5$  are five different target points. We use the maximum turning angle  $\alpha = \pi/6$  and the minimum leg length  $l = 50$  as the parameters for this test case. The target points are selected such that paths to each one have different number of turning points.

The numerical results are shown in Table 1 and the paths generated by the RCS and A\* algorithms for each target point are drawn in Figure 6(a-e). In each figure, the blue path is produced by RCS and the red one by A\*.

The first important fact derived from the results is that the running time of the A\* algorithm is much larger than the RCS algorithm. As it can be seen in Table 1, in this simple test case, the running time of A\* could be more than 10,000 times of the running time of RCS.

In the last column of Table 1 we show the relative difference between the length of paths generated by the algorithms. The relative difference is defined as  $100 \cdot |l_{\text{RCS}} - l_{\text{A}^*}| / \max\{l_{\text{RCS}}, l_{\text{A}^*}\}$ . In this formula,  $l_{\text{RCS}}$  and  $l_{\text{A}^*}$  are the length of the paths generated by RCS and A\*, respectively. As it can be seen, the relative difference between the length of paths produced by the algorithms is small, and in this experiment is always below 5%. Taking this into account and the fact that the running time of A\* is so huge compared to RCS, the effectiveness of our method becomes apparent.

Another outcome of this experiment is that as the number of obstacle vertices around which the path must turn increases, the running time of A\* increases too, whilst the running time of RCS is roughly constant. The increase in

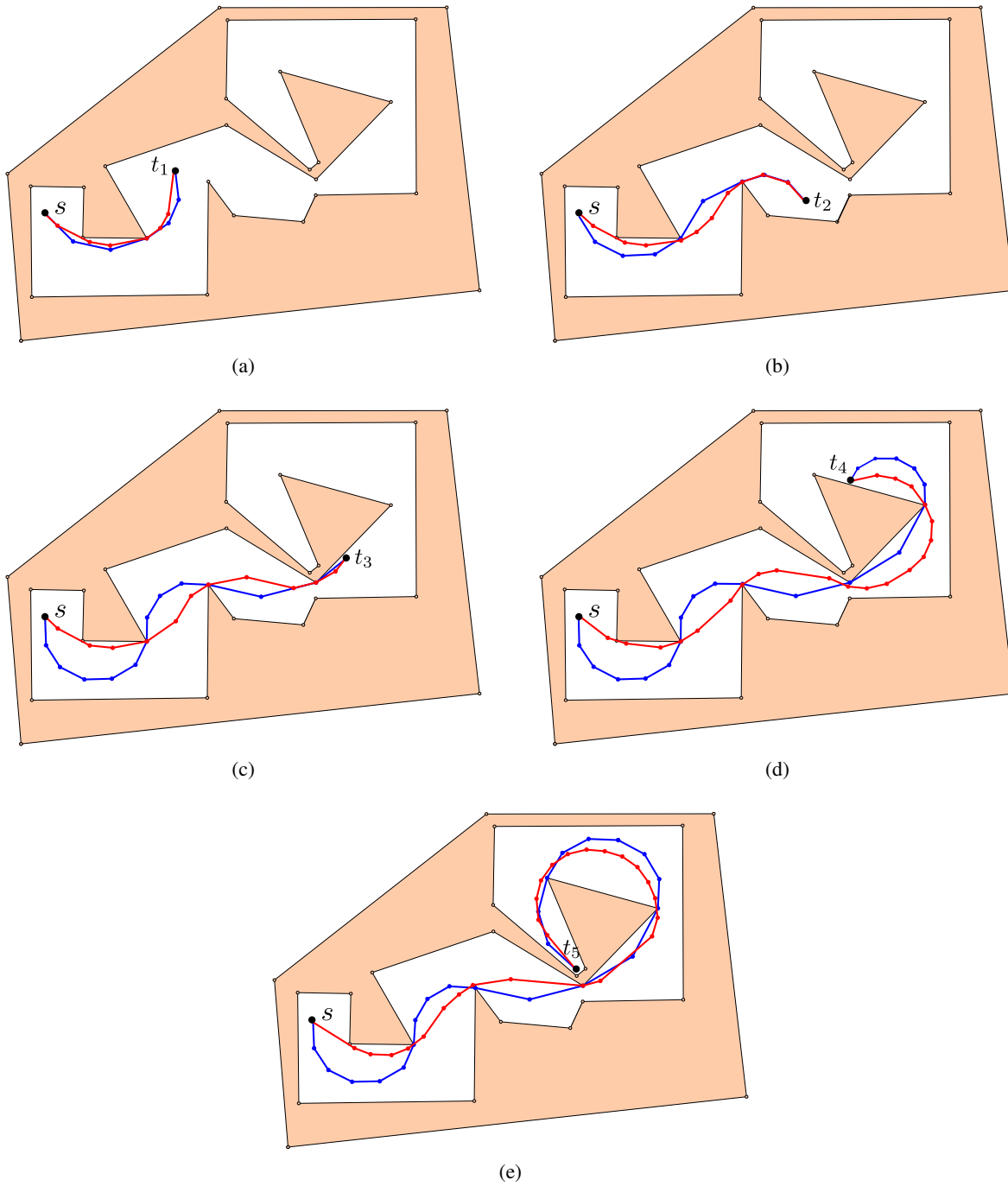


Figure 6: Demonstration of paths generated by the RCS (blue) and A\* (red) algorithms from  $s$  to  $t_1, \dots, t_5$ .

Table 2: Illustration of the effect of changing  $\alpha$  on the RCS and A\* algorithms.

Max. turning angle (degree)	RCS preprocessing time (ms)	RCS query time (ms)	RCS total time (ms)	A* running time (ms)	RCS path length	A* path length	Relative difference
80	0.20	0.44	0.64	119.8	466.1	477.6	2.4%
40	0.37	0.59	0.96	204.2	478.0	473.1	1.0%
20	0.16	0.68	0.84	1878.0	478.1	471.9	1.3%
10	0.18	0.48	0.66	5029.6	480.9	472.5	1.7%

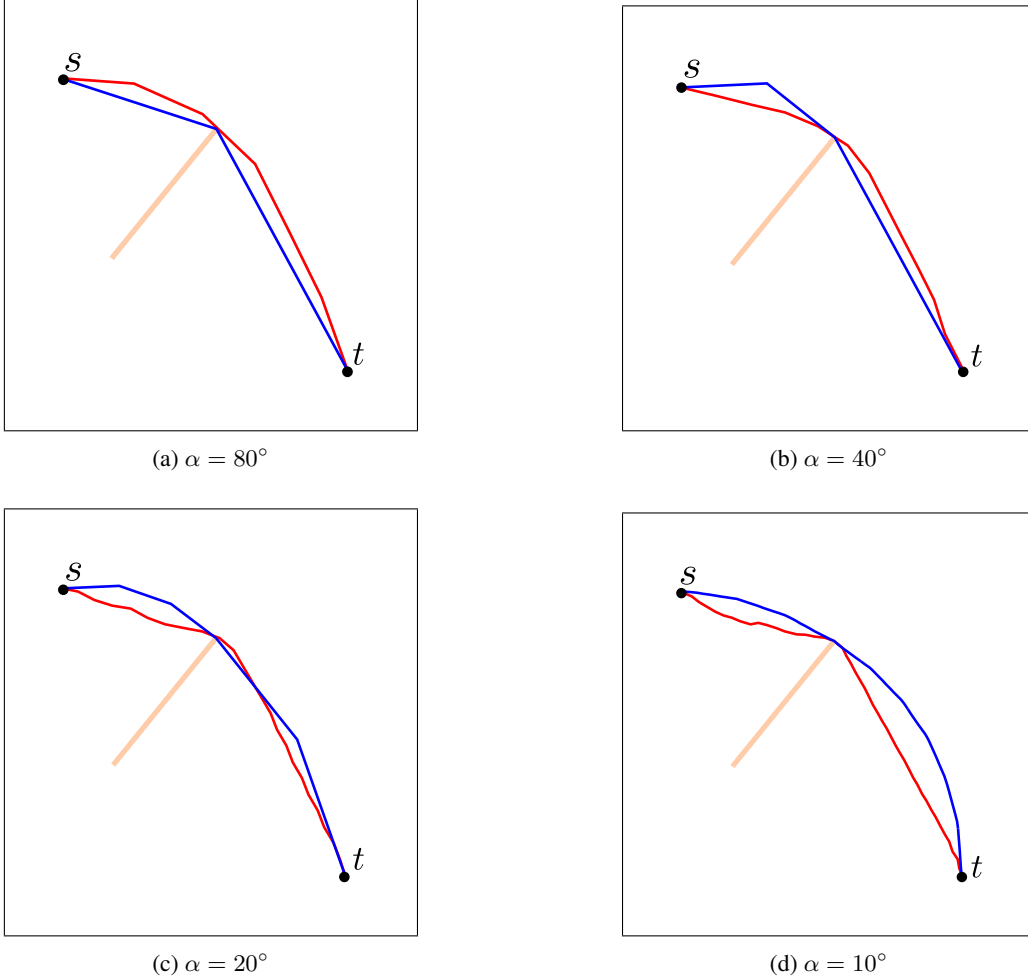


Figure 7: Demonstration of paths generated by the RCS (blue) and A\* (red) algorithms from  $s$  to  $t$  for different values of the maximum turning angle.

the running time of A\* might also be due to the increase in the path length, but as we will see in the subsequent experiments, the impact of this increase is negligible here.

In the second experiment, we intend to see the effect of changing the maximum turning angle parameter on the performance of the algorithms. We used a fixed simple scene of size  $400 \times 400$  consisting of a line segment as the only obstacle and two points as the starting and the target points. We chose  $l = 50$  as the minimum leg length, and 4 different values for the maximum turning angle, namely  $\alpha = 80, 40, 20, 10$ .

The numerical results are shown in Table 2 and the paths generated by RCS and A\* for each value of  $\alpha$  are drawn in Figure 7(a-d). As it can be seen from the table, the running time of the A\* algorithm dramatically increases as the maximum turning angle is decreased. On the other hand, the running time of RCS is not much dependent on the value of  $\alpha$ .

Table 3: Illustration of the effect of changing  $l$  on the RCS and A\* algorithms.

Min. leg length	RCS preprocessing time (ms)	RCS query time (ms)	RCS total time (ms)	A* running time (ms)	RCS path length	A* path length	Relative difference
40	0.16	0.72	0.88	121.7	279.2	283.3	1.4%
20	0.20	0.75	0.95	217.8	279.2	282.0	1.0%
10	0.22	0.73	0.95	554.4	279.2	281.9	1.0%
5	0.22	0.82	1.04	789.6	279.2	283.1	1.4%

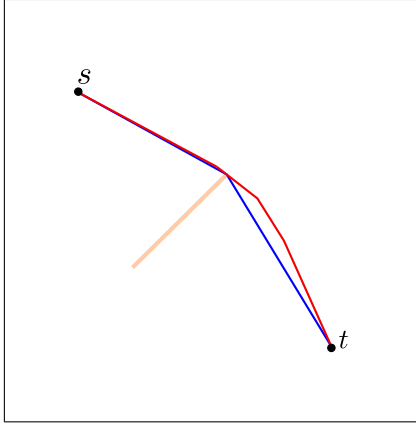
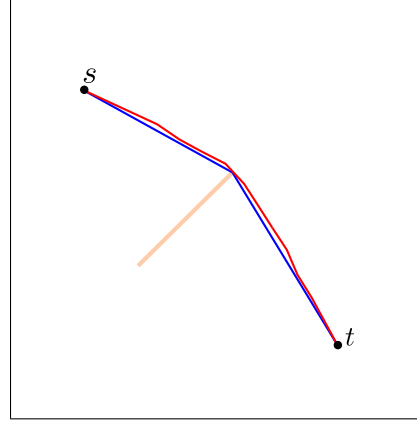
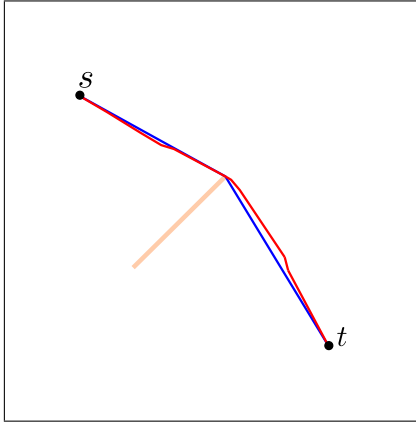
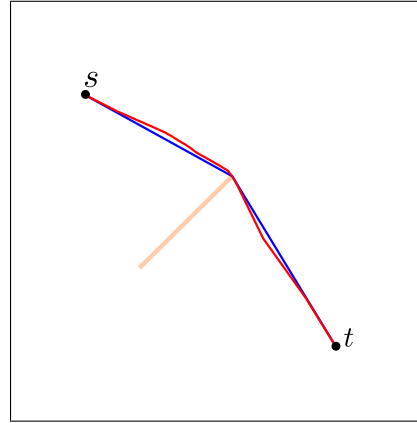

 (a)  $l = 40$ 

 (b)  $l = 20$ 

 (c)  $l = 10$ 

 (d)  $l = 5$ 

 Figure 8: Demonstration of paths generated by the RCS (blue) and A\* (red) algorithms from  $s$  to  $t$  for different values of the minimum leg length.

We carry out the next experiment to see the effect of changing the minimum leg length parameter on the performance of the algorithms. We used a fixed simple scene of size  $200 \times 200$  consisting of a line segment as the obstacle and two points as the starting and the target points. We chose  $\alpha = \pi/6$  as the maximum turning angle, and 4 different values for the minimum leg length, namely  $l = 40, 20, 10, 5$ .

The numerical results are shown in Table 3 and the paths generated by RCS and A\* for each value of  $l$  are drawn in Figure 8(a-d). As it can be seen from the figure, the paths generated by RCS are all the same, which is the shortest path with the given requirements. Furthermore, the running time of the A\* algorithm substantially increases as the minimum leg length is decreased. However, the running time of RCS is not much dependent on the value of  $\alpha$ .

In the fourth experiment, we want to illustrate the effect of increasing the complexity of the scene in terms of the number of vertices of obstacles. In this experiment, each scene consists of a fixed starting and a target point, and a set of rod-shaped obstacles. We double the number of obstacles in each scene. The maximum turning angle is selected as  $\alpha = \pi/6$ , and the minimum leg length as  $l = 50$ .

Table 4: Illustration of the effect of increasing the complexity of scene.

Test Case	#Obstacle	RCS preprocessing time (ms)	RCS query time (ms)	RCS total time (ms)	A* running time (ms)	RCS path length	A* path length	Relative difference
$t_1$	2	1.18	0.94	2.12	188.3	643.1	645.7	0.4%
$t_2$	4	6.56	1.18	7.74	149.6	643.2	645.8	0.4%
$t_3$	8	14.45	1.31	15.76	449.9	664.9	663.4	0.2%
$t_4$	16	33.08	2.07	35.15	318.8	747.3	669.1	10.5%
$t_5$	32	209.36	4.00	213.36	762.0	740.5	756.1	2.1%

Table 5: Illustration of the effect of changing size of the scene.

Test Case	Scene size	Minimum leg length	RCS prep. time (ms)	RCS query time (ms)	RCS total time (ms)	A* running time (ms)	RCS path length	A* path length	Relative difference
$t_1$	$100 \times 100$	10	0.22	0.77	0.99	182.2	141.6	143.4	1.26%
$t_2$	$200 \times 200$	20	0.27	0.79	1.06	233.2	284.7	287.6	1.01%
$t_3$	$400 \times 400$	40	0.23	0.80	1.03	455.0	570.8	574.5	0.64%
$t_4$	$800 \times 800$	80	0.22	0.80	1.02	1178.9	1143.0	1148.8	0.50%

Table 6: Illustration of the effect of the path length on the running time of RCS and A\*.

Path length	RCS preprocessing time (ms)	RCS query time (ms)	RCS total time (ms)	A* running time (ms)
100	0.0046	0.0159	0.0205	94.19
200	0.0046	0.0162	0.0208	104.21
400	0.0046	0.0174	0.0220	100.21
800	0.0046	0.0179	0.0225	95.73

The results are shown in Table 4 and Figure 9(a-e). From the results of the table, we see that the dependency of the running time of RCS is much greater to the complexity of the scene than A\*. Despite that, the running time of RCS is still less than the running time of A\*. The relative difference of the two algorithms are in most cases very small, and in three out of five cases, RCS found a path shorter than the path found by A\*.

In the fifth experiment, we show the effect of rescaling the workspace on the running time of the two algorithms. As illustrated in Figure 10 the scene consists of a fixed starting and a target point and a single rod-shaped obstacle. In each test case, we rescale the scene by doubling each coordinate, as well as the minimum leg length  $l$ . The maximum turning angle is selected as  $\alpha = \pi/6$ . It is obvious that with rescaling the scene, and the minimum leg length parameter, the path will not change.

The results are shown in Table 5. From these results we can easily conclude that the running time of A\* is greatly dependent on the size of the scene, while the running time of RCS is independent.

In the sixth experiment, we demonstrate the effect of path length on the running time of the algorithms. In this experiment, we use a simple scene consisting of only a starting point  $s$  and a target point  $t$ . The difference between each test case is the distance between the starting and the target points. In this experiment we choose  $l = 50$ , and  $\alpha = \pi/6$ . It is obvious that in this experiment the optimum path is simply the line segment from  $s$  to  $t$ .

The results of this experiment are shown in Table 6. From these results, it can easily be confirmed that the running time of the two algorithms is not dependent on the path length.

For the last experiment, we want to test the scalability of the RCS algorithm. We use six different polygonal domains of various sizes, and run the algorithm to find the required preprocessing and query time of the algorithm for each one. In these test cases, we choose the maximum turning angle  $\alpha = \pi/9$  and the minimum leg length  $l = 60$ . For each test case, the number of obstacles and vertices, and the preprocessing and query time in milliseconds are shown in Table 7.

One of the configurations used in this experiment is depicted in Figure 11. In this figure, a polygonal domain with 9 obstacles and 39 vertices is illustrated. The result of the algorithm on this configuration is shown when  $\alpha = \pi/18$  and  $l = 60$ .

## 7 Conclusion

In this paper we studied the problem of path planning for a robot with maximum turning angle and minimum leg length in a polygonal domain. We first proposed an algorithm to find a path avoiding obstacles with the aforementioned requirements. We then proved that the required space and the running time of the algorithm are  $O(n^4)$ . In order to decrease the path planning time, we further decomposed the algorithm into two parts, the preprocessing phase and the

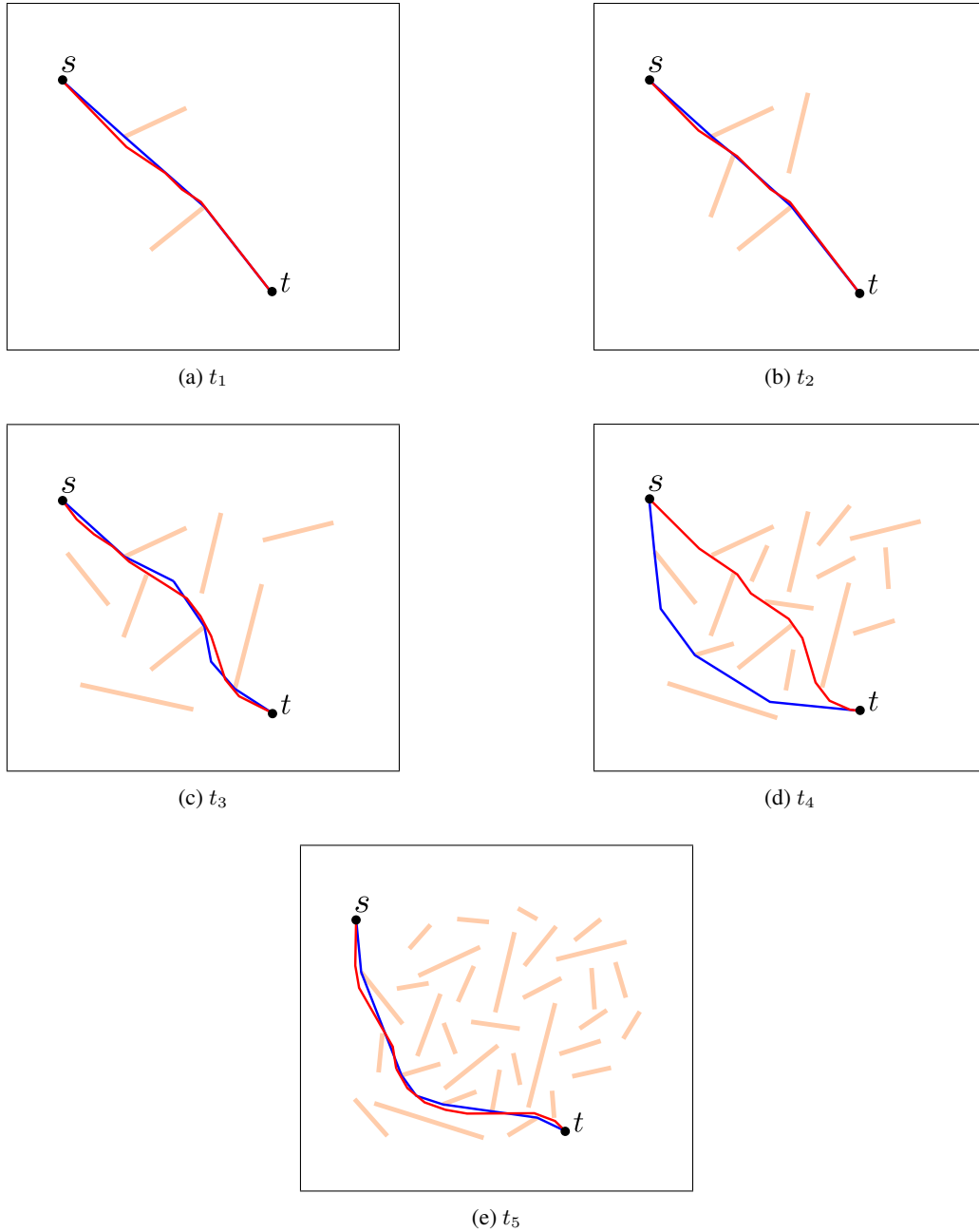


Figure 9: Demonstration of paths generated by the RCS (blue) and A\* (red) algorithms from  $s$  to  $t$  for scenes of different complexities.

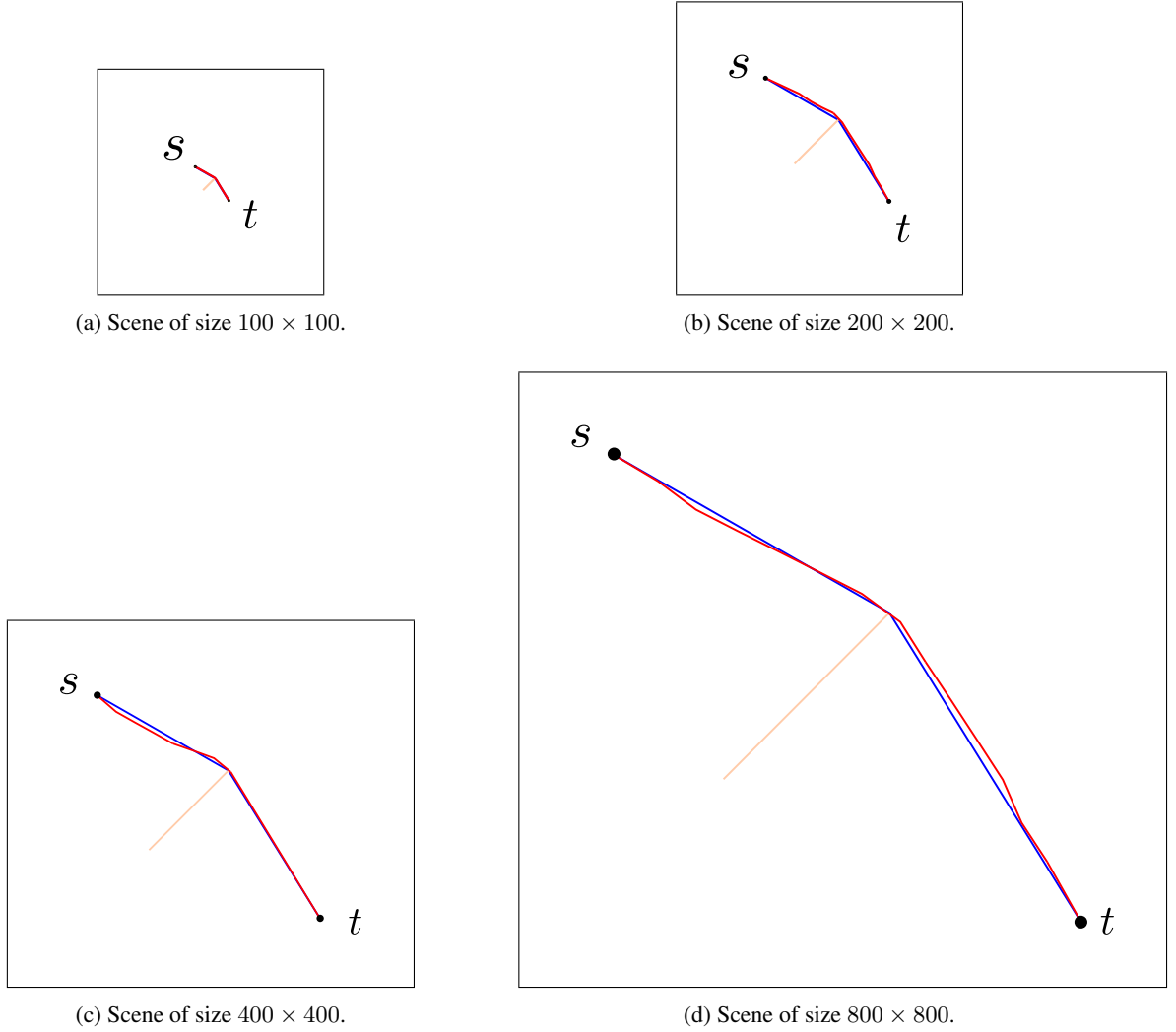


Figure 10: Demonstration of paths generated by the RCS (blue) and A\* (red) algorithms from  $s$  to  $t$  for scenes of different sizes.

Table 7: Preprocessing and query time of the RCS algorithm for scenes of various complexities.

Test case	#Obstacles	#Vertices	Preprocessing time (ms)	Query time (ms)
1	1	3	2	3
2	2	7	25	3
3	9	39	1166	18
4	26	100	2033	26
5	84	300	28860	188
6	180	500	223134	570

query phase. This helps to reduce the running time of the algorithm when a set of target points are going to be used in a fixed polygonal domain. In another extension, we changed the algorithm to answer path planning queries that require the object to approach the target from a given direction (or a range of directions).

Although our main goal was not to find the shortest path, as presented by the experiments, the solution is not much longer than the shortest path. Furthermore, comparing to most of the previous work on this problem, which uses heuristic and evolutionary methods, the running time of the algorithm is much less, and the algorithm is much scalable

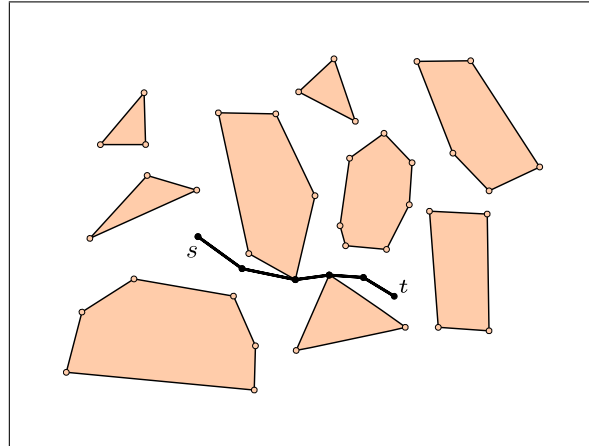


Figure 11: A polygonal domain with 9 obstacles and 39 vertices is illustrated in which we find a path with  $\alpha = \pi/18$  and  $l = 60$ .

to large complex environments. For future work, we try to improve the algorithm and find the shortest path with the given requirements.

## References

- [1] John Canny and John Reif. New lower bound techniques for robot motion planning problems. In *Foundations of Computer Science, 1987., 28th Annual Symposium on*, pages 49–60. IEEE, 1987.
- [2] Timothy M Chan. Optimal partition trees. *Discrete & Computational Geometry*, 47(4):661–690, 2012.
- [3] Danny Z Chen and Haitao Wang. Visibility and ray shooting queries in polygonal domains. *Computational Geometry*, 48(2):31–41, 2015.
- [4] Thomas H. Cormen, Charles E. Leiserson, Ronald L. Rivest, and Clifford Stein. *Introduction to Algorithms, Third Edition*. The MIT Press, 3rd edition, 2009.
- [5] Bruce Enderle. Commercial applications of uavs in japanese agriculture. In *AIAA 1st UAV Conference*, pages 2002–3400, 2002.
- [6] Yangguang Fu, Mingyue Ding, and Chengping Zhou. Phase angle-encoded and quantum-behaved particle swarm optimization applied to three-dimensional route planning for uav. *IEEE Transactions on Systems, Man, and Cybernetics-Part A: Systems and Humans*, 42(2):511–526, 2012.
- [7] Chad Goerzen, Zhaodan Kong, and Bernard Mettler. A survey of motion planning algorithms from the perspective of autonomous uav guidance. *Journal of Intelligent and Robotic Systems*, 57(1-4):65, 2010.
- [8] Katrina Herrick. Development of the unmanned aerial vehicle market: forecasts and trends. *Air & Space Europe*, 2(2):25–27, 2000.
- [9] Mangal Kothari, Ian Postlethwaite, and Da-Wei Gu. Multi-uav path planning in obstacle rich environments using rapidly-exploring random trees. In *Decision and Control, 2009 held jointly with the 2009 28th Chinese Control Conference. CDC/CCC 2009. Proceedings of the 48th IEEE Conference on*, pages 3069–3074. IEEE, 2009.
- [10] Steven M LaValle. *Planning algorithms*. Cambridge university press, 2006.
- [11] Jiří Matoušek. Range searching with efficient hierarchical cuttings. In *Proceedings of the eighth annual symposium on Computational geometry*, pages 276–285. ACM, 1992.
- [12] Shashi Mittal and Kalyanmoy Deb. Three-dimensional offline path planning for uavs using multiobjective evolutionary algorithms. In *Evolutionary Computation, 2007. CEC 2007. IEEE Congress on*, pages 3195–3202. IEEE, 2007.
- [13] Arman Nedjati, Gokhan Izbirak, Bela Vizvari, and Jamal Arkat. Complete coverage path planning for a multi-uav response system in post-earthquake assessment. *Robotics*, 5(4):26, 2016.
- [14] Ioannis Nikolos, Eleftherios Zografos, and Athina Brintaki. Uav path planning using evolutionary algorithms. *Innovations in Intelligent Machines-1*, pages 77–111, 2007.



- [15] Ioannis K Nikolos, Kimon P Valavanis, Nikos C Tsourveloudis, and Anargyros N Kostaras. Evolutionary algorithm based offline/online path planner for uav navigation. *IEEE Transactions on Systems, Man, and Cybernetics, Part B (Cybernetics)*, 33(6):898–912, 2003.
- [16] Mohammad Reza Ranjbar Divkoti. Astar path planning. <https://github.com/mrrranjbar/Astar-Path-Planning>, 2019.
- [17] Mohammad Reza Ranjbar Divkoti. Optimal path planning algorithm. <https://github.com/mrrranjbar/Optimal-Path-Planning-Algorithm>, 2019.
- [18] Mohammad Reza Ranjbar Divkoti and Mostafa Nouri-Baygi. Path planning in polygonal domains for robots with limited turning abilities. In *7th International Conference on Computer and Knowledge Engineering (ICCCKE), 2017*, pages 308–313, 2017.
- [19] John H Reif. Complexity of the mover’s problem and generalizations. In *Foundations of Computer Science, 1979., 20th Annual Symposium on*, pages 421–427. IEEE, 1979.
- [20] Vincent Roberge, Mohammed Tarbouchi, and Gilles Labonté. Comparison of parallel genetic algorithm and particle swarm optimization for real-time uav path planning. *IEEE Transactions on Industrial Informatics*, 9(1):132–141, 2013.
- [21] Ozgur Koray Sahingoz. Generation of bezier curve-based flyable trajectories for multi-uav systems with parallel genetic algorithm. *Journal of Intelligent & Robotic Systems*, 74(1-2):499, 2014.
- [22] Zak Sarris and S Atlas. Survey of uav applications in civil markets. In *IEEE Mediterranean Conference on Control and Automation*, page 11, 2001.
- [23] Robert J Szczerba, Peggy Galkowski, Ira S Glicktein, and Noah Ternullo. Robust algorithm for real-time route planning. *IEEE Transactions on Aerospace and Electronic Systems*, 36(3):869–878, 2000.
- [24] Naifeng Wen, Xiaohong Su, Peijun Ma, Lingling Zhao, and Yanhang Zhang. Online uav path planning in uncertain and hostile environments. *International Journal of Machine Learning and Cybernetics*, 8(2):469–487, 2017.
- [25] Naifeng Wen, Lingling Zhao, Xiaohong Su, and Peijun Ma. Uav online path planning algorithm in a low altitude dangerous environment. *IEEE/CAA Journal of Automatica Sinica*, 2(2):173–185, 2015.
- [26] Qian Xue, Peng Cheng, and Nong Cheng. Offline path planning and online replanning of uavs in complex terrain. In *Guidance, Navigation and Control Conference (CGNCC), 2014 IEEE Chinese*, pages 2287–2292. IEEE, 2014.
- [27] Kwangjin Yang and Salah Sukkarieh. 3d smooth path planning for a uav in cluttered natural environments. In *Intelligent Robots and Systems, 2008. IROS 2008. IEEE/RSJ International Conference on*, pages 794–800. IEEE, 2008.
- [28] Liang Yang, Dalei Song, Jizhong Xiao, Jianda Han, Liying Yang, and Yang Cao. Generation of dynamically feasible and collision free trajectory by applying six-order bezier curve and local optimal reshaping. In *Intelligent Robots and Systems (IROS), 2015 IEEE/RSJ International Conference on*, pages 643–648. IEEE, 2015.
- [29] Peng Yao, Honglun Wang, and Zikang Su. Cooperative path planning with applications to target tracking and obstacle avoidance for multi-uavs. *Aerospace Science and Technology*, 54:10–22, 2016.
- [30] Changwen Zheng, Mingyue Ding, and Chengping Zhou. Real-time route planning for unmanned air vehicle with an evolutionary algorithm. *International Journal of Pattern Recognition and Artificial Intelligence*, 17(01):63–81, 2003.
- [31] Changwen Zheng, Lei Li, Fanjiang Xu, Fuchun Sun, and Mingyue Ding. Evolutionary route planner for unmanned air vehicles. *IEEE Transactions on Robotics*, 21(4):609–620, 2005.